Summary

A case study for simulation of chloride transport in groundwater was carried out, in order to investigate methods and tools for prediction of pumped groundwater quality at drinking water wells. The case study concerns Pumping Station Roosteren, in Limburg Province.
First, a stationary groundwater flow model was constructed. Piezometric heads were simulated that represent average conditions between 1973 –1996. A relatively long period was selected, in order to maximize representativity of the constructed model for the variable conditions in the past years. By comparison of observed and simulated values, the model could be calibrated and its performance could be assessed. Calibration of the stationary flow model was carried out by application of a formalized, computer-based procedure that was developed within the framework of this project. Secondly, transient (time dependent) groundwater flow was simulated. By means of these simulations, additional calibration of river properties was carried out. Results of the calibrated transient flow model were used for simulation of chloride transport in the groundwater from 1983 to 1996.

Chloride concentrations
Chloride concentrations below 10 mg/l can be considered to occur in unpolluted groundwater. Close to surface elevation, observed chloride concentrations are relatively high, typically 50 – 70 mg/l. These high chloride concentrations are caused by agricultural production (fertiliser, manure) and by application of road salts during winter. Variability of chloride concentrations in time and space is high (20 – 110 mg/l) in these shallow sub-soil sections. Chloride concentrations in groundwater decrease in downward direction, resulting in values of 5 – 10 mg/l in sections below 20 m. below surface in the North-West part of the model area. In the South-East part, polluted water has infiltrated deeper, typically 20 – 50 m. b. s. Close to the River Meuse, chloride concentrations between 5 – 10 mg/l occur relatively close to surface elevation, near 5 m NAP. This is an indication of upward flow from deep groundwater sections towards the Meuse. The average of observed chloride concentrations in the Meuse at Stevensweert is 48 mg/l (1973-1996).
Close to the well screens of P.S. Roosteren, average chloride concentrations are 40 – 50 mg/l. Since 1983, chloride concentrations decreased at these locations. The observed decrease in chloride concentrations since 1983 is thought to be caused partly by reduced chloride deposition at the surface and partly by upconing of unpolluted groundwater due to groundwater abstraction at P.S. Roosteren.

Model results
The stationary calibration of the MODFLOW model resulted in an average absolute error of 0.22 m in layers above 0 m. NAP within the groundwater protection zone of P.S. Roosteren. Calibration was carried out by application of a computer based procedure that was specifically developed for this project. Average absolute *weighted*[1] errors in the same area are less than 0.10 m. Pathlines towards P.S. Roosteren were analysed by application of the MODPATH particle tracking code. A new stop criterion for weak sinks was added to this code, in order to improve results of the analyses of the origin of pumped water at P.S. Roosteren. The shape of the captive zone of P.S. Roosteren is relatively narrow and long. The greater part of the water presently being pumped at P.S. Roosteren infiltrated less than 25 years ago. A smaller part consists of infiltrated water from the River Meuse, with travel times of 1 – 2 years. A small part of the pumped water consists of relatively old and unpolluted water that passes through soil sections below 0 m NAP. At higher discharge rates at P.S. Roosteren, the relative contribution of water from the Meuse increases. According to the simulation results, the percentage of 'Meuse water' in pumped water at P.S. Roosteren would exceed 25 % at a discharge rate of 9 MM3/a.
Average errors in transient simulations within the groundwater protection zone of P.S. Roosteren are 0.01m.; average absolute errors are 0.49 m.
Simulation of chloride transport was carried out for 1983 –1996. Average absolute differences between observed and simulated chloride concentrations were less than 8 mg/l. These errors were regularly distributed over the simulation period.

[1] the weight of piezometric reference data was defined linear with the number of available data and inverse linear with the squared distance to a cell

General Project Data

Project title: PRESYS-GQ:
Demonstration of a Groundwater Quality Prediction System for Impact Assessment of Landuse Development on Sustainable Drinking Water Production
LIFE96ENV/NL/230

Project location: Pumping Station Roosteren
Region/country: Limburg Province, The Netherlands

Beneficiary's full name and address:

Utrecht University, Faculty of Geographical Sciences

P. O. Box 80.115, 3508 TC Utrecht

THE NETHERLANDS

Tel. (31)030-253.2359 fax. (31)030-253.2746

E-mail: p.schot@geog.uu.nl

Project manager: Dr. Paul P. Schot

Duration: 1-6-1997 - 1-6-2001 (48 months)

Total costs: 425,053.04 Ecu
Contribution by LIFE: 212,526.51 Ecu

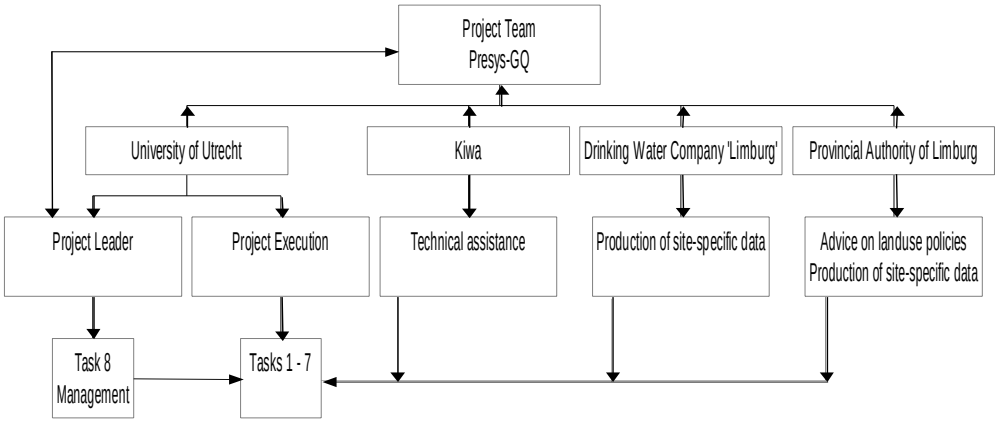

Organisational Structure

Figure 1: Organisation chart PRESYS-GQ Project.

Participants of the project:	**Tasks:**
- University of Utrecht	all main tasks;
- Kiwa	technical assistance, development of software modules;
- Drinking Water Company Limburg	production of site-specific data;
- Provincial Authority Limburg	advice on landuse policies, production of site-specific data.

Table of Contents

SUMMARY 1

GENERAL PROJECT DATA 3

ORGANISATIONAL STRUCTURE 4

TABLE OF CONTENTS 5

LIST OF FIGURES 6

LIST OF TABLES 6

LIST OF MAPS 7

1. INTRODUCTION 9

1.1. BACKGROUND 9
1.2. OBJECTIVES AND PROJECT PHASES 11
1.3. DESCRIPTION OF TASK 2 11
1.4. REPORT STRUCTURE 12

2. CONSTRUCTION OF THE FLOW MODEL 13

2.1. INTRODUCTION 13
2.2. DESCRIPTION OF MODEL PROPERTIES 15
2.2.1. Grid 15
2.2.2. Allocation of subsurface hydraulic properties 15
2.2.3. Recharge 16
2.2.4. Wells 20
2.2.5. River Meuse 20

3. CALIBRATION OF THE FLOW MODEL 22

3.1. MODELING APPROACH 22
3.2. CALIBRATION PROCEDURE 23
3.3. CALIBRATION RANGE OF MODEL INPUT VARIABLES 25
3.4. SIMULATION RESULTS BEFORE CALIBRATION 26
3.5. SIMULATION RESULTS AFTER CALIBRATION 27
3.6. PATHLINES 29

4. SIMULATION OF TRANSIENT GROUNDWATER FLOW 31

4.1. MODELLING APPROACH 31
4.2. SIMULATION RESULTS 32

5. SIMULATION OF CHLORIDE TRANSPORT 34

5.1. INTRODUCTION 34
5.2. OBSERVED CHLORIDE CONCENTRATIONS 34
5.2.1. River Meuse 34
5.2.2. Groundwater 34
5.3. MODELLING APPROACH 37
5.4. SIMULATION RESULTS 37
REFERENCES 40

APPENDICES 42

List of Figures

Figure 1: Organisation chart PRESYS-GQ Project. 4
Figure 2: Location of the model area 10
Figure 3: Schematic presentation of modelling approach 14
Figure 4: Calculated average annual recharge 18
Figure 5: Recharge fraction of precipitation; comparison of approaches 18
Figure 6: Production wells: Discharge of drinking water production wells in the model area 19
Figure 7: River Meuse: Annual averages of observed river stages 21
Figure 8: River Meuse: Monthly averages of observed river stages 1973-1996 21
Figure 9: Transient simulation: Comparison of simulated heads at P.S. Roosteren and observed heads at WP 33, at 40 m distance 33
Figure 10: Chloride: Annual averages of observed chloride concentrations in the River Meuse at Stevensweert 36
Figure 11: Chloride: Monthly averages of observed chloride concentrations in the River Meuse at Stevensweert 36
Figure 12: Chloride: annual averages of observed and simulated concentrations near P.S. Roosteren 39
Figure 13: Schematic presentation of components of the recharge model 45

List of Tables

Table 1: Thickness of model layers 15
Table 2: Allocated hydraulic properties of sediments 16
Table 3: Schematic presentation of the algorithm for adjustment of cell properties 25
Table 4: Calibration range factors of model input variables 26
Table 5: Stationary model performance before calibration: average model errors per layer 27
Table 6: Stationary model performance before calibration: average model errors per layer in groundwater protection zone 27
Table 7: Stationary model performance after calibration: average model errors per layer 28
Table 8: Stationary model performance after calibration: average model errors per layer in groundwater protection zone 28
Table 9: Water balance of the stationary model in MM3/a representing average conditions between 1973 - 1996 28
Table 10: Average difference of modified model input expressed as a fraction of applied calibration ranges 29
Table 11: Estimated contribution of water from the River Meuse to pumped groundwater at P.S. Roosteren at various discharge rates. 30
Table 12: Applied storage coefficients per model layer 31
Table 13: Transient model performance: average model errors per layer for the total simulation period (1973 – 1996) 32
Table 14: Transient model performance: average model errors per layer for the total simulation period (1973 – 1996) within the groundwater protection zone of P.S. Roosteren 32
Table 15: Groups of groundwater classes 45
Table 16: Landuse classes 45
Table 17: Cropfactors per landuse class and per decade 46
Table 18: Soil water retention capacity and critical z distance per soil class 46

List of Maps

Map 1: Horizontal Dimensions of the Grid 1
Map 2: Vertical Dimensions of the Grid, Cross section A – A' 2
Map 3: Vertical Dimensions of the Grid, Cross section B – B' 3
Map 4: Location of Boreholes with Available Lithological Descriptions 4
Map 5: Sub-soil Composition: Cross Section A – A' 5
Map 6: Sub-soil Composition: Cross Section B – B' 6
Map 7: Sub-soil Composition: Cross Section C – C' 7
Map 8: Sub-soil Composition: Cross Section D – D' 8
Map 9: Sub-soil Composition: Cross Section E – E' 9
Map 10: Stationary Calibration: Weighted Errors for Layer 1 10
Map 11: Stationary Calibration: Average Weighted Errors for Layer 2 – 8 11
Map 12: Stationary Calibration: Weighted Errors for Layer 9 12
Map 13: Stationary Calibration: Weighted Errors for Layer 10 13
Map 14: Stationary Simulation: Caption Zones of P.S. Roosteren at Various Discharge Rates 14
Map 15: Stationary Simulation: Pathlines towards P.S. Roosteren, Cross section C - C' 15
Map 16: Stationary Simulation: Destinations of Particles Released at the Groundwater Table, Location of Cross Sections 16
Map 17: Stationary Simulation: Destinations of Particles Released at 15 m. NAP (Elevation of well screens of P.S. Roosteren) 17
Map 18: Stationary Simulation: Destinations of Particles Released at 0 m. NAP 18
Map 19: Stationary Simulation: Destinations of Particles Released at -50 m. NAP 19
Map 20: Stationary Simulation: Destinations of Particles Released at -120 m. NAP 20
Map 21: Stationary Simulation: Destinations of Particles Released along Cross Section A – A' 21
Map 22: Stationary Simulation: Destinations of Particles Released along Cross Section B – B' 22
Map 23: Transient Simulation: Location of Reference Points with Presented Time-Head Graphs 23
Map 24: Chloride: Monitoring Wells with Measured Chloride Concentrations 24
Map 25: Chloride: Average Observed Concentrations 1983 - 1984 along Cross Section A – A' 25
Map 26: Chloride: Average Observed Concentrations 1991 - 1993 along Cross Section A – A' 26
Map 27: Chloride: Average Observed Concentrations 1994 - 1996 along Cross Section A – A' 27
Map 28: Chloride: Average Observed Concentrations 1997 - 1998 along Cross Section A – A' 28
Map 29: Chloride: Average Observed Concentrations 1983 - 1984 along Cross Section B – B' 29
Map 30: Chloride: Average Observed Concentrations 1991 - 1993 along Cross Section B – B' 30
Map 31: Chloride: Average Observed Concentrations 1994 - 1996 along Cross Section B – B' 31
Map 32: Chloride: Average Observed Concentrations 1997 - 1998 along Cross Section B – B' 32
Map 33: Chloride: Average Observed Concentrations 1983 - 1984 along Cross Section C – C' 33
Map 34: Chloride: Average Observed Concentrations 1991 - 1993 along Cross Section C – C' 34
Map 35: Chloride: Average Observed Concentrations 1994 - 1996 along Cross Section C – C' 35
Map 36: Chloride: Average Observed Concentrations 1997 - 1998 along Cross Section C – C' 36
Map 37: Chloride: Average Observed Concentrations 1983 - 1984 along Cross Section D – D' 37
Map 38: Chloride: Average Observed Concentrations 1991 - 1993 along Cross Section D – D' 38
Map 39: Chloride: Average Observed Concentrations 1994 - 1996 along Cross Section D – D' 39
Map 40: Chloride: Average Observed Concentrations 1997 - 1998 along Cross Section D – D' 40
Map 41: Chloride: Average Observed Concentrations 1983 - 1984 along Cross Section E – E' 41
Map 42: Chloride: Average Observed Concentrations 1991 - 1993 along Cross Section E – E' 42
Map 43: Chloride: Average Observed Concentrations 1994 - 1996 along Cross Section E – E' 43
Map 44: Chloride: Average Observed Concentrations 1997 - 1998 along Cross Section E – E' 44
Map 45: Chloride: Average Concentrations along Cross Section F – F' 1983 - 1984 45
Map 46: Chloride: Average Concentrations along Cross Section F – F' 1991 - 1993 46
Map 47: Chloride: Average Concentrations along Cross Section F – F' 1994 - 1996 47
Map 48: Chloride: Simulated Concentrations along Cross Section F – F' in 2060 48
Map 49: Stationary Calibration: Horizontal Hydraulic Conductivity of Layer 1 49
Map 50: Stationary Calibration: Average Horizontal Hydraulic Conductivity of Layer 2 - 8 50
Map 51: Stationary Calibration: Horizontal Hydraulic Conductivity of Layer 9 51
Map 52: Stationary Calibration: Horizontal Hydraulic Conductivity of Layer 10 52
Map 53: Stationary Calibration: Vertical Resistance of Layer 1 53
Map 54: Stationary Calibration: Vertical Resistance of Layer 8 - 9 54
Map 55: Stationary Calibration: Vertical Resistance of Layer 9 -10 55

1. Introduction

1.1. Background

This report forms part of the PRESYS-GQ project, which is focussed on the development of a groundwater quality prediction system. The project is being carried out by Utrecht University. Other project participants are Drinking Water Company Limburg (WML), Provincial Authorities of Limburg Province and Kiwa Onderzoek en Advies.

In the European Union, groundwater quality is deteriorating thus threatening the drinking water supply of tens of millions of people. One of the reasons groundwater contamination is still continuing, is the fact that local authorities (provincial and municipal) acting as land use planners, lack insight in the relation between different types of land use and their effects on groundwater quality. Therefore, local authorities generally disregard the need for sustainable (non-polluting) forms of land use in areas where groundwater contamination may lead to severe problems in drinking water wells.
On the other hand, drinking water companies generally lack insight in the future quality development of their primary source, i.e. groundwater. When a groundwater contamination is detected in water samples from monitoring or production wells, often rather ad-hoc decisions are made to invest either in purification facilities or in reallocation of wells, both of which are very costly. However, the long-term efficiency of these investments is unclear due to inadequate insight in future groundwater quality development.
In the light of the above there is an obvious need for a groundwater quality prediction system which can be used by the above mentioned actors relevant for the drinking water supply and which can facilitate an integrated decision making. This system should be accessible for experts as well as non-experts.
The prediction system will consist of an existing groundwater modelling package, which will be integrated with several new package modules. These new package modules will enable simulation of chemical processes in groundwater and soil, relevant to the production of drinking water. In this way, effects of different landuse policies on groundwater quality can be demonstrated. Simulation results will be presented by means of state-of-the-art computer visualisation techniques.
To demonstrate the feasibility of the prediction system a case study will be worked out for an area from the Province of Limburg, the Netherlands. Nonetheless, the prediction system will be designed for general purpose and will be applicable throughout the Community.

Figure 2 Location of the model area

1.2. Objectives and project phases

General objective of the PRESYS-GQ Project is the development of a groundwater quality prediction system which can be used by actors relevant for the drinking water supply and which can facilitate an integrated decision making. This system should be accessible for experts as well as non-experts.
The project consists of three phases. The relation between phases and tasks is described in the following paragraph.

A. Standard Model Construction
   - tasks 1, 2, 3
   - task 6 partly
B. Advanced model Construction
   - tasks 4, 5
   - task 6 partly
C. Dissemination
   - task 7
   - task 6 partly

In phase A the following tasks are distinguished:

1. Construction of a groundwater flow model (MODFLOW)
2. Construction of a conservative transport model for chloride (MT3D-Cl)
3. Standard non-conservative transport model (MT3D-decay)

This report pertains to the results of the aforementioned task 2.: Construction of a conservative transport model for simulation of chloride transport.

1.3. Description of task 2

Aim:
Simulation of conservative transport of chloride in the case-area.
Method:
1. Simulation of groundwater fluxes in the case area by means of the groundwater modelling software code MODFLOW.
2. Simulation of chloride transport in the case area by means of the groundwater transport software code MT3D96.
3. Chemical analyses of water samples.

Activities:
1. Collection of site-specific data on chloride deposition over time.
2. Collection of water samples for chemical analyses.
3. Simulation of groundwater fluxes over time after refining the groundwater model, which has been constructed during the execution of task 1. (MODFLOW).
4. Simulation of transport of chloride in the saturated zone over time (MT3D96).
5. Calibration of chloride transport by comparison of simulated with observed chloride concentrations.
6. Writing technical report T2.

Relation to other tasks:
The construction of the flow model during task 1 forms the basis for flow simulations of task 2.
The adapted flow model constitutes input for tasks 3,4,5 and 6.

1.4. Report structure

This report is divided in two parts. Part one contains the main text and a number of figures and tables. Part two contains maps and cross sections and is bound in a separate volume.
Chapter 1 of this report contains general information about the PRESYS-GQ project and a description of project progress. In Chapter 2, construction of the stationary groundwater model for simulation of average groundwater fluxes over 1973 – 1996 is described. Chapter 3 describes the calibration of the stationary flow model. Chapter 4 contains the description of transient simulations of groundwater flow in the model area. Chapter 5 describes the simulation of chloride transport through the saturated zone over time.

2. Construction of the Flow Model

2.1. Introduction

During task 1, the geohydrological characteristics of the case area have been investigated and a groundwater model has been constructed for simulation of piezometric head in the saturated zone. Results of these activities have indicated the relative importance of the various model variables. Thus could be concluded which factors were most indicated to be modified in order to improve model performance.

In this report, transport of chloride ions over time in groundwater will be described and simulated. In order to accomplish this task, the groundwater model, which has been constructed during task 1, was modified. There are two reasons why the initial groundwater model was adapted:

1. In order to prepare the model for simulation of groundwater *transport*
2. In order to improve model performance

The groundwater *flow* model (MODFLOW) not only generates output, such as simulated piezometric heads and groundwater fluxes that can be consulted directly, its results can also be used as input for a *tracer* model (Modpath) and a *transport* model (MT3D96).
A flow model that is meant to be used to generate input for tracer and transport models, has to be constructed with that objective in mind. A number of additional criteria exist in such a case. These criteria will be described in the course of this chapter**.** Figure 3 displays the scheme of simulations that are described in this report.

The principal adaptations of the groundwater model consider the items that are stated in the following:

- *Grid cell size*
- *Allocation of sub-surface hydraulic properties*
- *Calculation of recharge*
- *Allocation of river stages to cells*

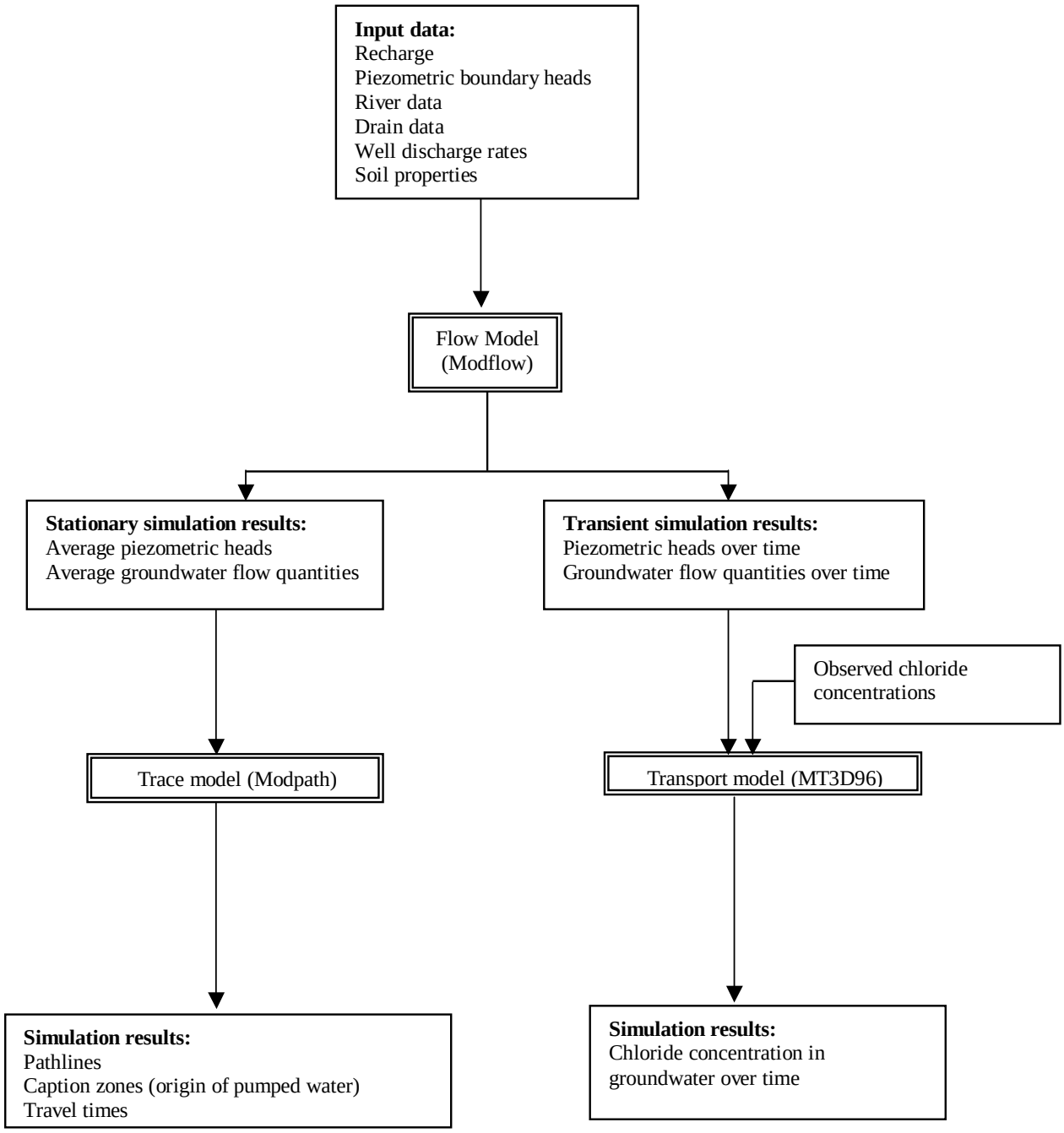

Figure 3: Schematic presentation of modelling approach

2.2. Description of model properties

As has been described in the introduction to this chapter, a number of modifications of the flow model was carried out. These modifications are partly according to the recommendations and conclusions of Technical Report 1, partly in order to meet the requirements of flow simulations for use by the transport model. In this paragraph, the adaptations will be described in more detail. For aspects of the flow model that have not been changed is referred to Technical Report 1.

2.2.1. Grid

Since sub-surface hydraulic conditions in the model area are highly variable (TR1), chemical interaction between subsoil and groundwater is thought to vary considerable within the caption zone of P.S. Roosteren. The cell sizes of the model need therefore to be smaller than would be required for simulation of piezometric heads only. Small cell sizes are also required in order to prevent pronounced *numerical dispersion*[2] during transport simulations.
The vertical delineation of layer boundaries does not coincide anymore with assumed boundaries of geological formations, as in Technical Report 1. It now consists for all layers but layer 1 of a *rectilinear* grid, in stead of a *distorted* grid in vertical direction. Layer 1 of the model still consists of distorted grid cells as to make the top of the model correspond to surface elevation. Due to the great variability of subsurface hydraulic properties, a 'distorted grid approach' would have lead to many layers with highly variable layer thickness, which often results in numerical instability of the model. Apart from numerical instability, a vertically distorted grid results in some error in the calculation of heads and fluxes (McDonald, M. G. & Harbaugh, A. W., 1984, pp 54).
A projection of the grid in the horizontal plane is displayed in Part 2 of this document (see Map 1). Cross sectional displays of layers are presented in Map 2 and Map 3.
The grid consists of 10 layers of 100 rows by 67 columns. The smallest grid cells, which are located around P.S. Roosteren, have a length and width of 50 m. In the vertical plane, the model consists of 10 layers with a layer thickness that increases in downward direction (see Table 1). Layer thickness of layer 9 and 10 are relatively large because changes in chloride concentrations of the groundwater insignificant in these two layers (see 5.2 Observed chloride concentrations).

Layer	Thickness (m)	Bottom layer elevation (m NAP)
1	5 – 40	20
2	1	19
3	2	17
4	2	15
5	2.5	12.5
6	3	9.5
7	4	5.5
8	5.5	0
9	60	-60
10	110	-170

Table 1 Thickness of model layers

2.2.2. Allocation of subsurface hydraulic properties

As a result of the relatively high level of detail that is required for transport simulations as compared to simulations of piezometric heads only, allocation of hydraulic properties of grid cells is based on lithological borehole descriptions. This method is different from the approach that was used in Technical Report 1, where estimates of aquifer *transmissivities* by TNO and the Geological Survey were used. In this study, initial allocation of horizontal and vertical hydraulic *conductivity* to grid cells is based on borehole descriptions that are available at Drinking Water Company Limburg (WML). Lithological characterisations from these descriptions have been linked to vertical and horizontal hydraulic conductivities, based on typical values as found in literature (Weerts, H. J. T.,1996, Todd, D.

[2] *Numerical dispersion* is caused by a too coarse model grid and results in simulation of unrealistic transport velocities of solutes.

K. 1980). The applied values are presented in Table 2. Horizontal and vertical hydraulic conductivities were calculated at locations where grid cells intersect with boreholes whose lithological descriptions were available. For remaining grid cells, values have been interpolated (linear inverse distance). Resulting cumulative transmissivities do not differ more than 10% from TNO estimates at sites where these are available. The locations of available data are presented in Map 4. A number of cross-sectional views of the subsoil in the model area are presented in Map 5 to Map 9. The maps clearly indicate the highly heterogeneous character of the subsoil in the model area. No borehole descriptions of deep boreholes around P.S. Roosteren are available. Available borehole descriptions do not describe sections below -10 m. NAP. Thus, lithological conditions below –10 m. NAP remain unknown in the West part of the model area. Upward flow from the deep subsoil around Roosteren towards the well screens depends largely on local vertical hydraulic conductivity. The presence of thick continuous layers of clay or brown coal would reduce such a flow almost completely, whereas its absence would lead to important groundwater fluxes of deep groundwater to P.S. Roosteren. Both scenarios are in principle possible, but they would lead to important differences in the chemical composition of pumped groundwater. Available descriptions of nearest-by located boreholes do not indicate the presence of thick, continuous clay layers between 0 – -30 m NAP.

Horizontal conductivity (m/d)	**Effective porosity (-)**	**Vertical conductivity (m/d)**	**Sediment description**
1	0.15	0.05	Small intermittent clay and sand layers
0.0005	0.15	0.0005	Brown coal
2.5	0.32	1	Fine sand
250	0.4	100	Pebbles
45	0.33	10	Coarse sand
0.001	0.05	0.001	Clay
0.05	0.1	0.005	Loam
12	0.3	5	Medium to coarse sand
45	0.3	20	Debris
0.01	0.05	0.01	Shell banks
0.05	0.35	0.01	Peat

Table 2 Allocated hydraulic properties of sediments

2.2.3. Recharge

During task 1, ground water flow simulations were performed for the year 1985. 1985 was a year with average precipitation and without significant dry periods. Therefore, actual evapotranspiration was assumed to equal potential evapotranspiration. The increase of the length of the simulation period that is required for the simulation of chloride transport, implies that a much greater variation of meteorological conditions occur. Periods with a significant water deficit included. Therefore the assumption that actual evapotranspiration would equal potential evapotranspiration (as in Technical Report 1) is no longer justified and a different technique for the calculation of net recharge has been adopted. With the newly adopted method, water balance calculations at a cell by cell basis have been carried out at decade intervals. The newly adopted approach consists of a so-called ‘basket’ model. If the calculated available soil moisture becomes low, actual evapotranspiration decreases. The applied recharge model is described in Appendix 2.

Applied data

Precipitation

Precipitation data on a decade (approx. 10 days) basis were used from meteorological stations Venlo, Echt, Buchten, Schinnen and Beek (see TR 1, Map 8). For each grid cell of the top layer of the model, precipitation values have been interpolated (linear inverse distance).

Potential evaporation

Penman potential evaporation data on a decade (approx. 10 days) basis were used from meteorological stations Venlo and Beek (see TR 1, Map 8). For each grid cell of the top layer of the model, potential evaporation values were interpolated (linear inverse distance) and subsequently multiplied by a time dependent cropfactor, associated with the dominant type of landuse in each grid cell. For a part of the calculation period, only *Makkink* evaporation data were available; these values have been converted to Penman values according to CHO-TNO publication No 19. (Anonymous, 1988).
Potential Penman evapotranspiration has been calculated by multiplication of potential evaporation values with the relevant cropfactor.

Penman cropfactors, depth of rootzone, interception

Cropfactors have been based on the dominant type of landuse for each grid cell, according to the digital landuse map as composed by DLO-SC Wageningen, linked with time-dependent cropfactors, based on CHO-TNO publication No 19. (Anonymous, 1988). Typical depths of rootzones and interception values have been based on values as found in literature (Anonymous, 1994).

Soil water retention capacity

Dominant soil types for each grid cell have been linked with soil water retention characteristics according to typical values as found in literature (Anonymous, 1994).

Groundwater class

The dominant groundwater class for each cell was determined by application of the digital soil map, as provided by DLO-SC Wageningen.

Supplementary irrigation during dry periods has not been accounted for in the recharge calculations.

Calculated recharge

Calculated recharge in Technical Report 1 for the year 1985 is virtually identical to the calculated annual average recharge according to the approach adopted in the current study. This is according to the expectations, as meteorological conditions in 1985 do not present pronounced dry periods. It can therefore be expected that potential evapotranspiration does not greatly differ from actual evapotranspiration.

Calculated recharge according to both approaches is presented in Figure 4. In general, recharge during dry periods is greater due a reduction of actual evapotranspiration as compared to potential evapotranspiration. In some cases, the newly adopted approach results in higher values of annual recharge as compared to the original approach. This is due to occurrence of capillary flow and to interpolation of precipitation values on a cell by cell basis in stead of application of an average value for all cells as was applied in Technical Report 1.

However, between 1973 and 1996 some much dryer periods than the year 1985 occur. For those conditions, calculated recharge based on the basket model differs considerably, since in the new recharge model actual evapotranspiration no longer equals potential evapotranspiration.
Calculated recharge amounts to 30% to 60% of the annual precipitation, measured at meteo stations Buchten and Echt, both located within the model area. The fraction of annual precipitation, which actually results in recharge according to both approaches, is displayed in Figure 5. In very dry years, the approach of T1 results in much lower values than the currently adopted approach.

Figure 4: Calculated average annual recharge

Figure 5: Recharge fraction of precipitation; comparison of approaches

Figure 6: Production wells: Discharge of drinking water production wells in the model area

2.2.4. Wells

Annual extracted volumes of groundwater by production wells for drinking water are presented in Figure 6. Annual discharges of wells within the model area were averaged per well location over the simulation period. If well screens penetrated more than one model layer, allocation of discharge rates to various layers was calculated proportionally to initial estimates of local horizontal transmissivity values of the intersected layers.

2.2.5. River Meuse

Average river stages have been calculated on a basis of daily stage observations at the available river gauge stations (see Technical Report 1, Map 8). Allocation of river stages to locations in between river stations have been performed according to three *stage relations curves*[3], provided by Rijkswaterstaat. In comparison with the linear inverse distance interpolation that was applied for task 1, use of stage relation curves resulted in local differences up to 0.3 m. It is assumed that the approach adopted in this study leads to more accurate results, since the hydraulic gradient is not constant along the river. The gradient also varies with river discharge rate. An accurate estimation of river stages near P.S. Roosteren is important to modelling results. River stages influence the fraction of water, which originates form the Meuse in the pumped groundwater at the pumping station.
Occasionally, riverbanks of the Meuse near the pumping station are flooded. Infiltration of Meuse water in the subsoil between the riverbed and P.S. Roosteren is not thought to be of importance for the chemical composition of the groundwater. Total average annual flood time is relatively short (a matter of days) and infiltration of river water is expected to be slow, due to low hydraulic conductivity of clays and loams that cover the river banks.
Seasonal variation of river stages varies more than 2 m. In this study, annual averages of river stages were used. The impact of short-term variation of river stages is thought to be insignificant for the chemical composition of groundwater between P.S. Roosteren and the Meuse. The impact of fluctuations of river stages on the representation of water that originates from the Meuse in pumped groundwater at Roosteren is thought to be linear over the range of short-term fluctuations of river stages. Thus, application of annual averages of river stages within model simulations should not lead to erroneous results. Travel times of water particles from the riverbank towards Roosteren exceed 6 months. Since all time-dependent input variables to the model consist of annual averages, model results cannot be evaluated at a time scale less than a year.

[3] A *stage relation curve* describes river stages as a function of discharge rate and location along a river.

Figure 7: River Meuse: Annual averages of observed river stages

Figure 8: River Meuse: Monthly averages of observed river stages 1973-1996

3. Calibration of the Flow Model

3.1. Modeling approach

Stationary and transient simulations
Simulations by numerical groundwater models can be carried out under stationary or transient conditions. Under stationary flow conditions, a situation of static equilibrium is assumed. In reality, a static equilibrium condition does hardly exist in most gravity-drained areas. However, it can be approached by averaging model-input variables over a long period. Then, time-dependent variables are assumed constant over the simulation period. A source of error is thus introduced into the simulation results since many model variables in reality are not constant during the simulation period. These variables often influence groundwater fluxes and piezometric head in a fashion that is not strictly linear.
For transient simulations, the equilibrium condition is no longer valid, but additional model parameters have to be defined (specific yield, storage coefficient), which increases the number of uncertain factors of the model. Model output also becomes time dependent and thus complicates evaluation of model performance.
Initial model simulations are therefore generally stationary. If transient simulation results are needed, they usually are carried out at second stage, after most model input has been calibrated under stationary conditions.

Calibration period
Calibration of time-independent hydraulic cell properties in this study has been carried out through simulation of stationary flow mainly, except for river conductivity. Values of model parameters which are in reality variable over time, such as recharge, piezometric boundary heads, pumping rates and river stages, have been averaged, in order to apply constant values for the stationary simulation. The stationary simulation represents average conditions between 1973 and 1996. River conductivity values have been calibrated through transient simulations, since river infiltration near P.S. Roosteren is caused by high well discharge rates. It does not occur in simulations of *average* stationary flow over the period 1973 – 1996. The considered time interval covers such a long period, in order to take a maximum of hydrological conditions in account. The groundwater that is being pumped up at P.S. Roosteren at present, was influenced by hydrological conditions of the last decades. Griffioen e.a. (1996) estimates that 1/3 of the pumped water at the well has an age of more than 25 years. One of the purposes of the current study is a reconstruction of conditions that determined the quality of the pumped water at P.S. Roosteren at present. The construction of models should therefore be based on a time span that represents the relevant hydro-chemical conditions correctly. The choice of the start of the simulation period (1973) was determined by data availability. Availability of data before 1973 was judged too small for use for the simulations.
The choice for use of data from a long period for stationary simulation implies that well discharges were not constant throughout the period. Averaging data from periods with different discharge rates is only justified if the impact of variable abstraction rates of production wells is linear proportional to the resulting drawdown. The non-linear impact of large differences in well's discharge rates over this period on piezometric heads is not expected to be very strong. Many wells are located in deep, confined aquifers, where it can be assumed that drawdowns are linear proportional to discharge rates. At P.S. Roosteren, groundwater is abstracted from a phreatic aquifer of high hydraulic transmissivity. Because of the high transmissivity in relation to discharge rates, drawdowns remain relatively small compared to saturated aquifer thickness. Non-linear infiltration from the drainage system is assumed limited since the drainage system in the area near P.S. Roosteren is mainly located in loamy sediments.
A supplementary advantage of calibrations based on long periods is that reaction times of piezometric heads to recharge that surpass a single hydrological season are thus also taken in account. The time it takes for excess of precipitation to enter the saturated zone depends on the thickness of the unsaturated zone and its moisture content. Reaction times may vary considerably from one place to another and from one period to another, but can easily surpass 6 months. In the case that a relatively short period of time would have been chosen as a basis for the stationary simulation, the possibility exists that meteorological conditions from before the considered period still largely influence piezometric head.

Adjustment of hydraulic conductivity's in order to match observed with simulated heads would thus lead to erroneous results.
Calibration has been carried out by application of a computer-based, formalised procedure, based on the principle that adjustment of model input variables should be evenly distributed, relative to their respective (user-defined) calibration ranges. After calibration of time-independent model variables, a validation of model performance has been carried out through a transient simulation, covering the period 1973 – 1996.

3.2. Calibration procedure

The calibration procedure that has been applied in task 1 has been modified in order to improve the estimates of hydraulic properties within the model area. However, the basic approach has remained the same.
Calibration has been carried out by application of a formalised, computer based procedure, which has been developed within the framework of the PRESYS-GQ project. The procedure is similar to the calibration technique as described in Technical Report 1 of this project (see TR1, 3.4). For every model variable that had been decided to be adjustable during calibration, a *calibration range*[4] was defined. Calibration of the model by this procedure results in *equal relative adjustment* of all model input variables in any cell with respect to the corresponding calibration ranges. The advantage of this method as compared to manual calibration consists in the application of consequent and explicit calibration decision rules. The calibration becomes thus reproducible. The basic decision rules do not differ significantly of those which are adopted by many groundwater modellers, but can be applied in a very gradual, piecemeal fashion, thanks to the brute force of present days computers. The ranges that determine the degree in which model input parameters can be adjusted are user-defined.

The procedure has been modified as compared to its application in Technical Report 1 with respect to two aspects, which are described in the following paragraphs:

1. Calculation of the error in any cell

In stead of a definition of a "target head" for every model cell by linear inverse distance interpolation of observed heads before calibration, as was used for automated calibration during task 1, in this study, an interpolation of *differences* between observed and simulated heads at reference points after every calibration cycle has been used for deciding whether the simulated piezometric head in a cell is either too high, too low, or correct.

$$E(i,j,k) = \frac{\sum [ER(r,k) * w(r,i,j,k)]}{N} * \frac{1}{\sum W(R,I,J,K)}$$

$$ER(r,k) = Hsim(i,j,k) - Href(i,j,k)$$

$$w = \sum [1 / d(r,i,j,k)^2 * ny(r)]$$

[4] A *calibration range* expresses how much model input variables are allowed to be modified in the course of the calibration process.

Where:

E:	Weighted error (m)
i,j,k:	Cell indexes: row, column, layer
ER :	Error in a reference cell (where observed heads are available)
r:	Index of reference cell
w:	Weight of error
n:	Number of reference heads
Hsim:	Simulated head
Href:	Annual average of observed head
d:	Distance
ny:	Number of years for which an average observed head could be calculated

The modification of the calibration procedure has been implemented since evaluation of the calibration procedure as applied in TR1 has indicated that results of spatial interpolation of piezometric heads are highly dependent on the type of interpolation technique that is applied. According to the modified procedure, calculation of error in any cell is entirely governed by calculated errors at reference points. Thus, the actual target head in a cell without reference data can actually remain undefined and only errors *at reference points* influence whether simulated head at any cell should increase or decrease.

2. Procedure for determination how input variables should be modified

Adjustment of input variables has been based on *a priori* relations between variables and simulated head. A schematic presentation of the applied algorithm is presented in Table 3**.**

Description	**Simulated head too low**	**Simulated head too high**
Variable	*Recharge*	
Conditions	-	-
Adjustment	Increase	Decrease
Variable	*drain level*	
Conditions	head >drain level	-
Adjustment	Increase	Decrease
Variable	*drain conductivity*	
Conditions	head >drain level	head >drain level
Adjustment	Decrease	Increase
Variable	*river level*	
Conditions	-	-
Adjustment	increase	Decrease
Variable	*river conductivity*	
Conditions	head >river level	head >river level
Adjustment	decrease	Increase
Conditions	head < river level	head < river level
Adjustment	Increase	Decrease
Variable	*horizontal hydraulic conductivity*	
Conditions	upstream too high, downstream too low	upstream too low, downstream too high
Adjustment	Increase	Decrease
Variable	*vertical hydraulic conductivity*	
Conditions	underlying layer head too high	underlying layer head too low
	underlying layer head higher	underlying layer head lower
Adjustment	increase	Decrease
Conditions	underlying layer too high	underlying layer too low
Conditions	underlying layer head lower	underlying layer head lower
Adjustment	decrease	Increase

Table 3 Schematic presentation of the algorithm for adjustment of cell properties

3.3. Calibration range of model input variables

The determination of calibration ranges was based on data availability, data variability and best professional judgement. Additional data collection and a modified schematisation of the hydrological system have lead to an adjustment of calibration ranges, which are presented in Table 4. Two types of calibration ranges have been used: a relative scale, which defines the limits as a fraction of the initial value and an absolute range. The latter has been applied for calibration of drain levels.

Relatively and absolutely defined calibration ranges Rr and Ra are defined according to:

$V_{max} = E + Rr * E$ $\quad\quad$ $V_{max} = E + Ra$

$V_{min} = E - Rr * E$ $\quad\quad$ $V_{min} = E - Ra$

In the case of vertical hydraulic conductivity, it has been considered necessary to increase the size of the calibration ranges to more than 1. In those cases, the lower limit of the calibration range of hydraulic resistance has been set at 0.00001 d^{-1} in order to prevent calculation of negative values. Large calibration ranges for vertical hydraulic conductance values are necessary because estimates are highly uncertain. The presence or absence of layers of clay, or brown coal, within a section of subsoil may influence resulting vertical hydraulic conductivity with several orders of magnitude. Uncertainty of vertical conductivity is particularly high for layers 9 and 10 (thickness of respectively 60 and 110 m), where no borehole descriptions are available in large parts of the model area.

A is defined according to:

$$A = \frac{(V - E)}{2 * Rr * E}$$

In the case of absolute ranges (drain levels)

$$A = \frac{(V - E)}{2 * Ra}$$

where:
A: Deviation factor (–0.5>=A<=0.5)
V: Calibrated value of a model input variable
E: Initial value of a model input variable
Rr: Calibration range factor, relative to E (user defined)
Ra: Calibration range factor in units of the variable (user defined)

Availability of lithological borehole descriptions becomes scarcer with increasing depth, which explains the manifest increase of calibration ranges with depth below surface.

		Layer									
Variable	**Units**	**1**	**2**	**3**	**4**	**5**	**6**	**7**	**8**	**9**	**10**
Thickness	M	**5 - 40**	**1**	**2**	**2**	**2.5**	**3**	**4**	**5.5**	**60**	**110**
Horizontal conductivity	-	0.8	0.5	0.5	0.5	0.5	0.5	0.5	0.5	0.8	0.8
Vertical conductivity	-	2	0.8	0.8	0.8	0.8	0.8	0.8	5	5	-
Drain levels	M	0.5	-	-	-	-	-	-	-	-	-
Drain conductivity	-	0.5	-	-	-	-	-	-	-	-	-
River conductivity	-	0.5	0.5	0.5	0.5	-	-	-	-	-	-
Recharge	-	0.4	-	-	-	-	-	-	-	-	-

Table 4 Calibration range factors of model input variables

3.4. Simulation results before calibration

Piezometric simulation results before calibration are presented in Table 5 and Table 6. Negative errors indicate simulated heads are lower than averages of observed values. Relative high errors occur

in model layers 1, 9 and 10, which is partly caused by the high thickness of these layers: differences of observed piezometric heads within upper and lower parts of these layer may vary considerably. Average simulated heads tend to be too low in the eastern part of the model area, whereas in the western part simulated heads are too high, in comparison with mean observed values at reference boreholes.

Layer	Average error (m)	Average absolute error (m)	Average weighted [5] error (m)	Number of reference points
1	-0.03	0.70	0.10	203
2	0.12	0.46	0.11	130
3	0.10	0.40	0.09	153
4	0.21	0.36	0.19	132
5	0.20	0.40	0.20	149
6	0.26	0.39	0.26	113
7	0.24	0.36	0.21	98
8	0.27	0.45	0.30	81
9	1.65	2.80	1.62	251
10	0.72	1.52	0.78	98

Table 5 Stationary model performance before calibration: average model errors per layer

Layer	Average error (m)	Average absolute error (m)	Average weighted error (m)	Number of reference points
1	0.15	0.44	0.19	96
2	0.09	0.32	0.14	75
3	0.08	0.30	0.14	99
4	0.19	0.33	0.18	89
5	0.22	0.34	0.22	103
6	0.23	0.38	0.24	76
7	0.14	0.30	0.14	68
8	0.23	0.41	0.24	61
9	2.68	3.25	2.63	99
10	0.92	1.70	1.01	43

Table 6 Stationary model performance before calibration: average model errors per layer in groundwater protection zone

3.5. Simulation results after calibration

After calibration of the model by modifying input values of model variables, model errors have decreased. Errors per layer are displayed in Table 7 and Table 8; a spatial presentation of model performance can be seen in Map 10 to Map 13 . The weighted errors, which are displayed in the aforementioned maps, have been calculated according to the formula described in 3.2. Model results within the groundwater protection zone of P.S. Roosteren are better than in remote areas of the model, which may be due to scarce availability of data in the latter areas. Simulated heads in model layers 9 and 10 vary more from observed values than other model layers. Because of the great thickness of these layers, piezometric head may vary significantly between top and bottom of these layers. Screens that are located within these layers typically only penetrate a small part of the total layer thickness and therefore rarely represent average conditions.

[5] The weight of a reference point is linear to the number of years for which a representative annual average piezometric head could be calculated and inverse linear with the squared distance of any cell to a reference point.

Layer	Average error (m)	Average absolute error (m)	Average weighted error (m)	Number of reference points
1	-0.07	0.39	-0.06	203
2	-0.01	0.33	-0.02	130
3	-0.02	0.28	-0.01	153
4	0.05	0.23	0.05	132
5	0.05	0.26	0.05	149
6	0.07	0.24	0.08	113
7	0.09	0.25	0.07	98
8	0.08	0.32	0.08	81
9	1.66	2.63	1.65	251
10	0.77	1.51	0.77	98

Table 7 Stationary model performance after calibration: average model errors per layer

Layer	Average error (m)	Average absolute error (m)	Average weighted error (m)	Number of reference points
1	0.00	0.27	-0.01	96
2	0.02	0.21	0.01	75
3	0.01	0.18	0.02	99
4	0.04	0.19	0.04	89
5	0.06	0.22	0.07	103
6	0.03	0.23	0.05	76
7	-0.01	0.19	-0.01	68
8	0.00	0.24	-0.01	61
9	2.38	3.00	2.39	99
10	0.98	1.70	1.05	43

Table 8 Stationary model performance after calibration: average model errors per layer in groundwater protection zone

Simulated groundwater fluxes cannot be compared directly with field observations. Since the model area consists of generally of aquifers with high horizontal transmissivity values, small differences in simulated piezometric gradient lead already to high changes in corresponding groundwater fluxes. Given the importance of flow, rather than head, to processes related to groundwater quality, within the framework of this study a correct simulation of fluxes is decisive. The principal validation of simulated groundwater fluxes consists in the evaluation of results of the transport model.
In Table 9, the average annual water balance in the model area is presented, according to results of the calibrated stationary model. At P.S. Roosteren

Source or Sink	Model in	Model out
Recharge	50	0
Drains	0	16
Wells	0	9
River Meuse[6]	13	40
Boundaries	55	54
Total	118	118

Table 9 Water balance of the stationary model in MM3/a representing average conditions between 1973 - 1996 .

[6] Infiltrated water from the River Meuse consists of bypass flow near meanders and ends up in other parts of the river. The average discharge rate of P.S. Roosteren over the period 1973-1996 is too low to induce important infiltration of river water towards the well.

Table 10 indicates to which degree model input variables have been modified during calibration, expressed in a factor named A. A may vary between –0.5 and 0.5, respectively corresponding to the lower and upper limit of the calibration range.
At A=0 the average value of a variable corresponds with its value before calibration.

The stated values represent average and absolute average values of A per layer, per model input variable.

	Layer									
Variable	1	2	3	4	5	6	7	8	9	10
KHOR	0.00	0.02	0.02	0.02	0.02	0.02	0.02	0.02	0.00	0.02
KHOR (abs)	0.05	0.05	0.05	0.05	0.05	0.05	0.05	0.05	0.04	0.03
VCON	-0.09	0.00	0.00	0.00	0.00	0.00	0.00	0.07	-0.17	-
VCON (abs)	0.08	0.00	0.00	0.00	0.00	0.02	0.04	0.14	0.20	-
DRNP	-0.19	-	-	-	-	-	-	-	-	-
DRNP (abs)	0.23	-	-	-	-	-	-	-	-	-
DRNC	0.20	-	-	-	-	-	-	-	-	-
DRNC (abs)	0.22	-	-	-	-	-	-	-	-	-
RIVC	0.06	0.05	0.05	0.05	-	-	-	-	-	-
RIVC (abs)	0.06	0.05	0.05	0.05	-	-	-	-	-	-
RCHE	-0.06	-	-	-	-	-	-	-	-	-
RCHE (abs)	0.46	-	-	-	-	-	-	-	-	-

Table 10 Average difference of modified model input expressed as a fraction of applied calibration ranges

3.6. Pathlines

Analyses of pathlines was carried out by means of the particle tracking code MODPATH (Pollock, 1994). Particle tracing was carried out by forward tracing of randomnly distributed particles at various elevations. Destinations of randomly distributed particles at several depths have been calculated at a discharge rate at P.S. Roosteren of 6 MM3/a. Other model input values remained as during calibration runs (1973 – 1996 averages). Results of these calculations are presented in
Map 16 to Map 22. Indicative calculations of the captive zone of P.S. Roosteren were carried out for abstraction rates of 2 and 9 MM3/a (see Map 14). Traced particles that were released at the water table indicate that the shape of the captive zone of P.S. Roosteren is relatively narrow, in comparison with the delineation of the provincial groundwater protection zone. The narrowness is due to relatively high transmissivity values together with pronounced regional gradients as compared to the simulated abstraction rates. Given the poor data availability for the extreme South East part of the model area, the delineation of the captive zone in this part of the model area should be interpreted with reserve. The

numerical representation of drains in the model is not very detailed, which implies relatively high levels of uncertainty with respect to results of particle tracking. The calculations were carried out with application of a modified 'stop criterion' in cells with *weak sinks*[7]. In order to improve results of particle tracing in cells with weak sinks, a modification of the source code of MODPATH was implemented, within the framework of the PRESYS-GQ Project. The standard functionality of MODPATH was extended with an option which enables the apllication of a stop criterion that is governed by probability. The actual probability is determined by the relative magnitude of the weak sink, as compared to the total cell flux. The choice between the available options within the MODPATH code for handling model cells with 'weak sinks' has a very strong impact on the results of the calculations.
In Map 15, a cross sectional impression of groundwater flow towards P.S. Roosteren is presented. Cross sectional presentations of destinations of released particles are presented in Map 21 and Map 22. The cross sectional maps show that some groundwater from below 0 m NAP (layer 9) ends up in the River Meuse and P.S. Roosteren. This is not only caused by extraction at P.S. Roosteren, but also a result of the regional flow pattern. Piezometric heads in aquifers below 0 m NAP are higher than the head in the phreatic aquifer in the section above 0 m. NAP in the West part of the model area. The actual size of the upwards directed groundwater flux near the River Meuse depends greatly on vertical conductivity of the sub-soil. Higher pumping rates at P.S. Roosteren will result in an increase of flow from subsoil sections below 0 m NAP towards the well.The images do not contain information on the relative contribution of the various model layers to pumped water at P.S. Roosteren, since groundwater flow velocities vary among model layers. Calculation of the fraction of pumped groundwater at P.S. Roosteren that comes from the Meuse is highly depended on allocated river conductivity values. As will be discussed more in detail in Chapter 4, calibration of river conductivities has been carried out through transient simulations. Because of the high sensitivity of results to allocated river conductivity, estimations of the fraction of Meuse water in pumped water at P.S. Roosteren remain rather uncertain. The results of the calculations have been enumerated in Table 11.

Discharge rate at P.S. Roosteren (MM3/a)	**Minimal contribution(%)**	**Maximal contribution (%)**
2	0	35
6	7	45
9	25	60

Table 11 Estimated contribution of water from the River Meuse to pumped groundwater at P.S. Roosteren at various discharge rates.

[7] Cells with *weak sinks* are cells where a part of the calculated fluxes leaves the model; e.g. cells with drains or draining rivers.

4. Simulation of Transient Groundwater Flow

4.1. Modelling approach

After calibration of the stationary model, simulation of transient flow was carried out for the period 1973 – 1996. In stead of application of long term averages of model variables, as has been done for stationary flow simulations, in this case annual averages of time dependent variables have been used for model input. These input values concern wells' abstraction rates, river stages, recharge rates and model boundary heads. The total simulation period consists of 24 different *stress periods*[8] with each a period length of one year.
Additional input data that is required for transient simulation of groundwater flow are storage coefficients and specific yield. Confined storage factors have been estimated according to Lohman (1972):

S = 3*10E-06 * B

Where B represents saturated aquifer thickness (m). Resulting values for storage coefficient S are presented in Table 12. No value for layer 1 has been stated since layer 1 is unconfined. Specific yield data of lithological entities within the model area have been based on Weerts (1996) and Todd (1980) (see Table 2, effective porosity). Values have been allocated to model cells according to available borehole description data and linear inverse distance interpolation per model layer.

Model layer	Saturated thickness (m)	Storage coefficient (-)
1	1 – 40	
2	1	0.000003
3	2	0.000006
4	2	0.000006
5	2.5	7.5E-06
6	3	0.000009
7	4	0.000012
8	5.5	1.65E-05
9	60	0.00018
10	110	0.00033

Table 12 Applied storage coefficients per model layer

River conductivity values for the River Meuse have been calibrated through transient simulations. The discharge rate allocated to P.S. Roosteren during stationary calibration represented average discharge from 1973 – 1996 and therefore resulted in a low value (see Figure 6). Under these conditions, no significant quantities of water infiltrated towards the pumping station from the River Meuse. At high discharge rates at P.S. Roosteren conditions for calibration of river bed properties are more favourable, as in those conditions simulated piezometric heads are much more sensitive to river conductivity. Simulated heads near P.S. Roosteren were before calibration of riverbed conductivity more than 1.5 m. too low at the highest discharge rates at P.S. Roosteren. Differences between observed at simulated heads decreased considerably by increasing river conductivity. Model performance after calibration will be discussed in the following paragraph.

[8] A stress period is a period during which model input remains constant

4.2. Simulation results

Table 13 displays average model errors per layer over the total simulation period. In Table 14 errors within the groundwater protection zone of P.S. Roosteren are presented.

Layer	1	2	3	4	5	6	7	8	9	10	All
Average error (m)	-0.57	-0.16	-0.06	0.01	0.01	0.11	0.10	-0.14	0.74	0.50	-0.03
Average absolute error (m)	0.81	0.37	0.36	0.39	0.41	0.42	0.34	0.48	1.83	1.42	0.69

Table 13 Transient model performance: average model errors per layer for the total simulation period (1973 – 1996)

Layer	1	2	3	4	5	6	7	8	9	10	All
Average error (m)	-0.03	-0.13	-0.08	-0.04	-0.10	-0.13	-0.09	-0.19	0.85	0.43	0.01
Average absolute error (m)	0.27	0.28	0.28	0.32	0.31	0.31	0.24	0.26	1.22	1.64	0.49

Table 14 Transient model performance: average model errors per layer for the total simulation period (1973 – 1996) within the groundwater protection zone of P.S. Roosteren

A comparison of observed and simulated heads in time at P.S. Roosteren is displayed in Figure 9. In this figure, simulated heads at P.S. Roosteren can be compared with the nearest monitoring well (WP 33). Both individual observations and annual averages of observed heads are displayed, in order to illustrate the impact that application of annual averages has at the results. WP 33 is located at about 40 m. SSW from P.S. Roosteren.
Graphs for other monitoring wells are presented in Appendix 4.
General model performance corresponds well with averages of observed piezometric heads for most periods. Especially in the South-East part of the model area, piezometric heads in soil sections below 0 m. NAP have decreased 3 – 5 m. from 1980 – 1992. This cause of this decrease is unknown and is assumed to be located outside the model area. Simulated heads are influenced through a decrease of piezometric boundary heads.
Which particular model input variable should be corrected for further improvement of simulation results cannot be determined directly from the flow model. A reduction of errors by increment of applied calibration ranges is possible, but it is not evident that further adjustments of model input should improve reliability of modelling results. The process of model calibration contains an immanent risk of *'over calibrating'*, or introducing errors in order to compensate for other errors. If, for instance, erroneous values of boundary heads are the main reason for model errors, a compensation of these errors by adjustment of hydraulic conductivity would not result in a 'better' model: simulated heads might correspond closer to observed values, but errors in simulated groundwater fluxes would become worse. In such a case, it is not likely that simulation results of groundwater transport modelling also would improve.

Figure 9: Transient simulation: Comparison of simulated heads at P.S. Roosteren and observed heads at WP 33, at 40 m distance

5. Simulation of Chloride Transport

5.1. Introduction

Prediction of nitrate concentrations in pumped groundwater at P.S. Roosteren forms a major target of this project[9]. It may not seem evident how a study of the transport of chloride ions could possibly contribute to a better understanding of the occurrence of nitrates in groundwater. Contrary to nitrate, the occurrence of chloride in groundwater at concentrations as observed in the caption zone does not limit the possibilities for the production of drinking water, indeed sometimes chlorine is added in order to prevent bacteriological contamination. Similarly, the chemical behaviour of both ions in the subsoil is entirely different. Chloride ions are largely inert, whereas nitrate can react with many solids and solutes that occur in the soil.

However, deposition of chloride and nitrate over the last four decades display in general a similar increase in deposited quantities, as both are strongly related to changes in agricultural production. In rural areas, low concentrations of chloride correspond with groundwater that originates from before the time that agricultural production became industrialized.

Since chloride ions, contrary to nitrate, are chemically almost inert, it offers a possibility to simulate the transport of groundwater solutes without the complication of biodegradation. The process of biodegradation frequently affects nitrate concentrations and therefore adds a degree of freedom to prediction uncertainty. Thus, chloride can be used as a natural tracer with respect to groundwater flow. Low chloride concentrations point to unpolluted, often relatively old water. Nitrate concentrations in unpolluted water are also low.

Results of the transient flow simulations have been used for simulation of chloride transport by a MT3D96 transport model (Papadopoulos et al., 1990,1991).

This chapter will start with a presentation of observed chloride concentrations in the model area, followed by a description of the modelling approach and results of transport simulations.

5.2. Observed chloride concentrations

5.2.1. River Meuse

Sources of data

Chloride analyses of water from the Meuse have been supplied by Rijkswaterstaat Maastricht.

Data availability

Available chloride concentrations in the River Meuse that have been used in this study have been measured at Stevensweert, located at the North corner of the model area. Samples at this site have been analysed about every 2 weeks, from 1975 onwards. Total number of available analyses is 445.

Description

Observed values are displayed in Figure 10 and 11. Annual averages vary between 33 and 70 mg/l. Concentrations are strongly related to river discharge rate. Annual averages may vary more than 20 mg between adjacent years and no clear trend is distinguishable. The average value of the chloride concentrations at Stevensweert is 48 mg/l.

5.2.2. Groundwater

Sources of data

Observations on chloride concentrations in groundwater have been supplied by Waterleiding Maatschappij Limburg (WML) and Rijks Instituut Voor Milieu onderzoek (RIVM). An overview of these data has been supplied by Olde Wolbers (1998).

[9] Simulation of nitrate transport will be discussed in Technical Reports 3 and 4

Data availability

Similar to piezometric head data, the major part of the available data on chloride concentrations is located at the western part of the model area. All available data is located in the Dutch part of the model area (see Map 24). The total number of analyses amounts to 726, measured between 1969 – 1998 at 202 different screens. From these, 634 records have been sampled at locations within the model area. Long series of data at any location are scarcely available; many screens have only been analysed once or twice, which limits possibilities to determine developments of chloride concentration in time. Appendix 3 displays availability of data over time.

Spatial variation

Observed chloride concentrations within the model area vary from 4.4 to 110 mg/l. In general, chloride concentrations tend to decrease with sample depth below surface elevation. This is consistent with the increase of pollution in time and the general feature that the time that passed since water infiltrated increases with depth below the surface. In Map 26 to Map 38, cross-sectional presentations of chloride concentrations are displayed. The presented cross sections both cover periods that correspond to pumping and non-pumping conditions at Roosteren, as pumping at P.S. Roosteren started in 1985. Clearly can be seen that chloride concentrations decrease with increasing depth below the surface. Chloride concentrations below 10 mg/l indicate that the groundwater is unpolluted. Near P.S. Roosteren, there exists a stable, sharp transition between polluted and unpolluted water, near 0 – 10 m NAP. This indicates upward flow from deep groundwater towards the Meuse and P.S. Roosteren.

Variation in time

Variation of observed chloride concentrations at depths greater than 30 m. below the surface only display very gradual changes. Typically, these differences do not exceed 2 mg/l/year. Observation points near the surface show often highly variable chloride concentrations, because at these locations the response to deposition at the surface is much more direct than at deeper sites, where temporary impacts have been damped by the transport process. Chloride deposition at the surface is a rather discontinuous phenomenon, as application of fertiliser and road salts is not regularly distributed over time. Presented chloride concentrations in Map 26 to Map 38 that are located close to the surface should therefore interpreted with care. Generally, only few (1 – 3) observations are available per screen per presented period in these cross sectional maps and therefore representativity is limited for screens that are located less than 10 m below the surface. The significance of differences in chloride concentration between groundwater samples that originate from deeper located screens are assumed to be more significant, as a result of the aforementioned dampening impact of the transport process on temporal variations in chloride concentration. In general, observed chloride concentrations near P.S. Roosteren have decreased since 1983.

Figure 10: Chloride: Annual averages of observed chloride concentrations in the River Meuse at Stevensweert

Figure 11: Chloride: Monthly averages of observed chloride concentrations in the River Meuse at Stevensweert

5.3. Modelling approach

With respect to P.S. Roosteren, chloride concentrations indicate to which degree the groundwater originates from deep aquifers with relatively old groundwater or from shallow aquifers with relatively young water. Simulation of chloride transport can thus be used for validation of simulation results of the flow model. If simulated chloride concentrations correspond with observed chloride concentrations, this is an indication that the origin of simulated fluxes by the flow model corresponds to the real fluxes.
Simulation of chloride transport has been carried out on a basis of a transient simulation of the flow model (see Chapter 4). The simulation period is 1983 – 1996. Since data availability on chloride concentrations is very poor, no satisfactionary level of reliability could be achieved for allocation of chloride concentrations to model cells for the period before 1983. However, the simulation run starts before pumping started at P.S. Roosteren (1985) and enables to evaluate the impact of pumping at P.S. Roosteren on chloride concentrations in the groundwater. Time dependent conditions within the flow model concern annual averages of well discharges, river stages, recharge rates and boundary heads.
In order to assess chloride loads at the surface, detailed calculations of the chloride balance between 1970 and 1996 were carried out at Kiwa Environmental Consultants, by Beekman and Otte (1997). The study of Otte was carried out within the framework of the PRESYS-GQ Project, funded by LIFE-EC. Transport of chloride in the unsaturated zone was simulated by means of the REGIONIT code (Beekman, 1996). The major sources of chloride are:

1. agricultural production (application of manure, fertiliser)
2. road maintenance (application of road salts against formation of ice)
3. atmospheric deposition

The major sink of chloride consists of harvesting agricultural products.
The results of the study of Beekman and Otte showed that an accurate calculation of chloride loads that enter the saturated zone is not feasible. Quantities of both sinks and sources of chloride are very large as compared to the quantities of chloride that actually enter the groundwater system. No accurate data are available on applied quantities of fertiliser and of chloride concentrations of harvested products. Therefore, small errors in calculations of the quantities involved in the sinks and sources of chloride result in large errors. Calculations carried out by Otte resulted frequently in negative values of infiltrated chloride mass. This clearly indicated that the level of accurracy of the calculations is insufficient for use of the results in further calculations of chloride transport in groundwater. In this study, estimations of chloride quantities within the groundwater system were therefore based upon observed chloride concentrations.
Cells in layer 1, 9 and 10 of the model were set at a constant chloride concentration. Allocation of starting values to cells with constant concentrations was based on average observed concentrations during the simulation period. Time dependent allocation of concentrations to cells of layer 1 would represent the real conditions much more adequatly than the 'time independent' approach that was adopted. However, very poor data availability did not permit a reliable reconstruction of chloride loads at the water table over time. Therefore, allocated values to layer 1 were based at averages of observed values between 1983 and 1996. Values for cells have been calculated by linear inverse distance interpolation per model layer.
Calculated chloride concentrations in cells in layer 2 – 8 varied during the simulation. Allocation of initial chloride concentrations to these model cells corresponds to average conditions in 1983 to 1984. Observed data from the year 1984 were added, since for 1983 alone too few chloride observations were available. River cells that represent the River Meuse, were allocated annual averages of observed chloride concentrations at Stevensweert. Influence of hydrodynamic dispersion was not taken in account. As observed gradients of chloride concentrations are relatively low and data availability poor, no reliable calibration of dispersion was feasible.

5.4. Simulation results

Evaluation of simulation results is limited to observations in model layers 2 – 8, since other model layers were allocated constant concentrations. Thus, model performance has been compared with 290 observations. Average differences between observed and simulated chloride concentrations in the model area are –4 mg/l. Absolute differences amount to 8 mg/l. Standard deviation of the error is 12.3 mg/l. About 50% of all errors are between –6 and 6 mg/l. A graphical presentation of observed and simulated chloride concentrations versus time at P.S. Roosteren is displayed in Figure 12. Similar graphs at other locations are presented in Appendix 5. In Map 45 to Map 47, results of the simulations with MT3D are presented in conjunction of averages of observed values in monitoring wells. Clearly can be seen that the general model results correspond well with observed chloride concentrations. As

allocated concentrations to layer 1 of the model had to remain constant because of poor data availability, impacts of varying chloride loads at the water table are not represented in the model. Below the screens of P.S. Roosteren an upward flow from unpolluted groundwater can be observed. Observed chloride concentrations in monitoring wells WP 261-3, WP11-3 and WP9A-3 display observed concentrations of 8 mg/l and less, which indicates the presence of unpolluted groundwater. The unpolluted groundwater flows towards the River Meuse as a result of natural groundwater flow. Pumping at P.S. Roosteren, which started in 1985, caused an increase of upward flow. The observed chloride concentrations in the aforementioned monitoring wells decreased since 1985, which confirms these model results.

Map 48 displays simulated chloride concentrations in 2060. It was assumed that the discharge rate at P.S. Roosteren was 5.8 MM3/a. Other wells in the model area were allocated rates according to 1987. Other model variables represent 1973 –1996 averages. Chloride concentrations in the River Meuse were set at 40 mg/l. The results show a decrease of chloride concentrations in groundwater directly below P.S. Roosteren as a result of further upconing of unpolluted groundwater from sub-soil sections below 0 m. NAP. In the South-East direction from the well, chloride concentrations in layer 9 (0 - -60 m NAP) have increased, presumebly caused by downward flow from layers above 0 m NAP towards the screens of P.S. Susteren.

Figure 12: Chloride: annual averages of observed and simulated concentrations near P.S. Roosteren

References

Anonymous, (1976). *Rapport betreffende de Geologische Gesteldheid en de Hydrogeologishe Verhoudingen in het Gebied Roosteren – Koeweide.* Rijks Geologische Dienst Geologisch Bureau voor het Mijngebied, Heerlen

Anonymus, (1988). V*an Penman naar Makkink.* CHO-TNO, No. 19.

Beekman, W. (1997). *REGIO-NIT Modelbeschrijving; Regionaal Model voor de Simulatie van de Stikstofbelasting aan Maaiveld, onder de Wortelzone en op het Grondwater.* Kiwa Onderzoek en Advies SWE 97.002, Nieuwegein.

Griffioen, J., Laeven, M. P., Stuyfzand, P.J. (1997). *Selektie van de Studielokaties voor het Testen van het Geïntegreerd Transportmodel.* NITG-TNO, Kiwa Onderzoek en Advies.

Homan, M. (1974). *Grondwaterkaart van Nederland; voorlopige resultaten geohydrologische verkenning Roerdalslenk.* DGV TNO, Delft

Homan, M., Lekahena, E. G. (1977). *Grondwaterkaart van Nederland; inventarisatie rapport Sittard.* DGV TNO, Delft

Kragt, J. F., Juhász-Holterman, M. H. A. (1992). *Onderzoek naar de Gevolgen van de Oevergrondwaterwinning te Roosteren.* N.V. Waterleiding Maatschappij Limburg.

Lohman, S. W. (1972). *Groundwater Hydraulics.* US Department of Interior/US Geological Survey Prof. Paper 708, Reston, USA

McDonald, M. G. & Harbaugh, A. W. (1984). *A Modular Three-Dimensional Finite-Difference Groundwater Flow Model.* US Department of Interior/US Geological Survey, Reston, USA

Papadopoulos, S.S. et al. (1990,1991). MT3D, *A Modular Three-Dimensional Transport Model.* S.S. Papadopoulos & Associates Inc., Rockville, Maryland, USA

Olde Wolbers, M. J. (1998) *Beschrijving van de Grondwaterkwaliteit in het Intrekgebied van Pompstation Roosteren.* Waterleiding Maatschappij Limburg/Universiteit Utrecht, Maastricht.

Otte, J. (1998) *Stikstof- en Chloridebelasting Ondiep Grondwater rondom Roosteren.* Kiwa Onderzoek en Advies, SWI 98.129, Nieuwegein.

Pollock, D. W. (1994) *Modpath version 3: A particle Tracking Post-Processing Package for MODFLOW, the U.S. Geological Survey Finite-Difference Ground-water Flow Model.* US Geological Survey, Reston, USA

Stuurman, R. J., Pakes, U. (1991). *Hydrologische Systeemanalyse Noord- en Midden-Limburg.* TNO-GG, Delft

Stuurman, R. J. et al. (1996). *Landelijke Hydrologische Systeemanalyse; deelrapport 5.* TNO-GG, Delft

Todd, D. K. (1980). *Groundwater Hydrology.* John Wiley & Sons, New York, USA.

Weerts, H. J. T. (1996). *Complex Confining Layers*; architecture and hydraulic properties of Holocene and Late Weichselian deposits in the fluvial Rhine-Meuse delta, The Netherlands, Utrecht University, Utrecht.

Appendices

Appendix 1 Time Table of the PRESYS-GQ Project

Appendix 2 Calculation of Recharge

Recharge model description

Recharge has been calculated on a cell-by-cell basis, according to a simplified water balance model. Reservoirs that corresponded with the grid of the groundwater model could collect precipitation and allow recharge, if the reservoir is filled.

R	=	f(mc,Pn)
Mc	=	f(swrc,dr,cfl)
Pn	=	P-Ea-I
Ea	=	f(mc,ETP)
ETP	=	EP*cf
Cfl	=	f(gc,zc)
Zc	=	f(sc)

Where

R:	recharge
Ea:	actual evapotranspiration
ETP:	potential evapotranspiration
EP:	Penman portential evaporation
cf:	Penman crop factor
mc:	moisture content
Pn:	net precipitation
P:	precipitation
I:	interception
swrc:	soil water retention capacity
dr:	depth of rootzone
Cfl:	potential cappilary flux
gc:	groundwater class
zc:	critical z distance
sc:	soil class

A schematic presentation of the relevant processes is presented in Figure 13. For consultation of the applied classes and parameter values, see Table 15 to Table 18.

Supplementary irrigation during dry periods has not been accounted for in recharge calculations since no experimental data on this item are available. Direct run off has not been taken in account in the calculations of recharge; it forms thus an unknown part of the calculated ‘recharge’ sum, which has been taken in account during the calibration process by comparison with discharge quantities of the drainage system.

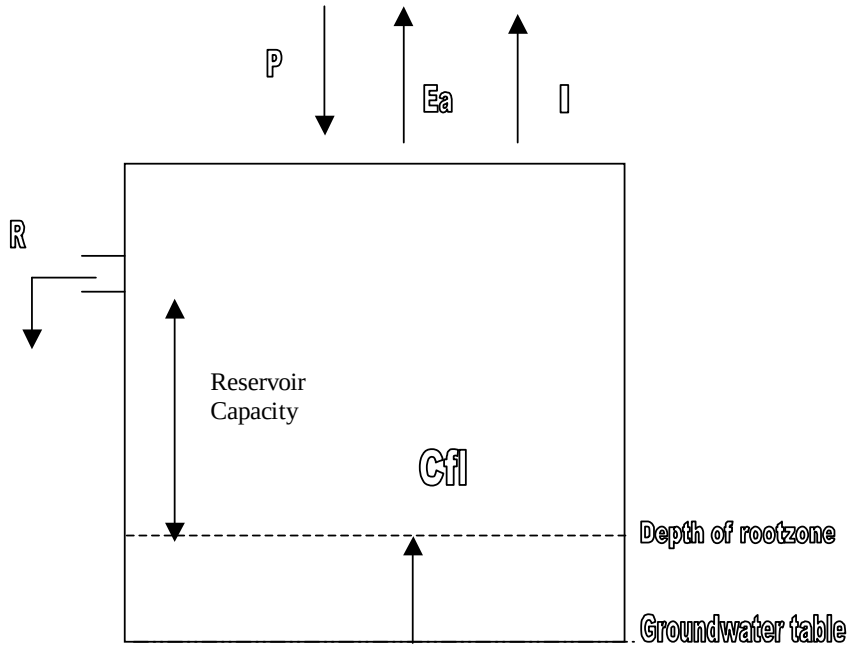

Figure 13 Schematic presentation of components of the recharge model

Class-groups	glg[10] (m.b.s.)	Groundwater classes DLO-SC
1	0.4	I
2	0.7	II, IIb
3	1	III, IIIb, IV
4	>1	>IV

Table 15: Groups of groundwater classes

Number	Landuse class
1	Cereals
2	Potatoes
3	Beets
4	Bulbs
5	Maize
6	Grass
7	Fruit trees
8	Deciduous forest
9	Pine forest
10	Water
11	Bare soil
12	Rest arable
13	Urban

Table 16: Landuse classes

[10] glg: Average lowest depth of water table

Table 17: Cropfactors per landuse class and per decade

Dec [11]	Land use classes												
	1	**2**	**3**	**4**	**5**	**6**	**7**	**8**	**9**	**10**	**11**	**12**	**13**
1	0.3	0.3	0.3	0.3	0.3	0.6	0.3	0.3	0.6	0.9	0.4	0.3	0.5
2	0.3	0.3	0.3	0.3	0.3	0.6	0.3	0.3	0.6	0.9	0.4	0.3	0.5
3	0.3	0.3	0.3	0.3	0.3	0.6	0.3	0.3	0.6	0.9	0.4	0.3	0.5
4	0.3	0.3	0.3	0.3	0.3	0.6	0.3	0.3	0.6	0.9	0.4	0.3	0.5
5	0.3	0.3	0.3	0.3	0.3	0.6	0.3	0.3	0.6	0.9	0.4	0.3	0.5
6	0.3	0.3	0.3	0.3	0.3	0.6	0.3	0.3	0.6	0.9	0.4	0.3	0.5
7	0.3	0.3	0.3	0.3	0.3	0.6	0.3	0.3	0.6	0.9	0.4	0.3	0.5
8	0.3	0.3	0.3	0.3	0.3	0.6	0.3	0.3	0.6	0.9	0.4	0.3	0.5
9	0.3	0.3	0.3	0.3	0.3	0.6	0.3	0.3	0.6	0.9	0.4	0.3	0.5
10	0.5	0.3	0.3	0.3	0.3	0.8	0.8	0.8	0.8	0.9	0.4	0.34	0.5
11	0.6	0.3	0.3	0.3	0.3	0.8	0.8	0.8	0.8	0.9	0.4	0.36	0.5
12	0.7	0.3	0.3	0.3	0.3	0.8	0.8	0.9	0.9	0.9	0.4	0.38	0.5
13	0.8	0.3	0.4	0.3	0.4	0.8	1.1	1	1	0.9	0.4	0.44	0.5
14	0.8	0.5	0.4	0.4	0.5	0.8	1.1	1.1	1.1	0.9	0.4	0.52	0.5
15	0.8	0.7	0.4	0.5	0.6	0.8	1.1	1.1	1.1	0.9	0.4	0.6	0.5
16	0.9	0.8	0.6	0.5	0.7	0.8	1.2	1.2	1.2	0.9	0.4	0.7	0.5
17	0.9	0.8	0.8	0.7	0.8	0.8	1.2	1.2	1.2	0.9	0.4	0.8	0.5
18	0.9	0.9	0.9	0.9	0.9	0.8	1.2	1.2	1.2	0.9	0.4	0.9	0.5
19	0.8	0.9	0.9	0.9	1	0.8	1.3	1.3	1.3	0.9	0.4	0.9	0.5
20	0.7	0.9	0.9	0.9	1	0.8	1.3	1.3	1.3	0.9	0.4	0.88	0.5
21	0.6	0.9	0.9	1	1	0.8	1.3	1.2	1.2	0.9	0.4	0.88	0.5
22	0.5	0.9	0.9	1	1	0.8	1.1	1.1	1.1	0.9	0.4	0.86	0.5
23	0.4	0.7	0.9	1	1	0.8	1.1	1.1	1.1	0.9	0.4	0.8	0.5
24	0.3	0.7	0.9	1	1	0.8	1	1.1	1.1	0.9	0.4	0.78	0.5
25	0.3	0.6	0.9	1	1	0.8	1	1	1	0.9	0.4	0.76	0.5
26	0.3	0.4	0.9	1	1	0.8	1	1	1	0.9	0.4	0.72	0.5
27	0.3	0.3	0.9	1	1	0.8	1	0.6	0.8	0.9	0.4	0.7	0.5
28	0.3	0.3	0.3	0.3	0.3	0.6	0.3	0.3	0.6	0.9	0.4	0.3	0.5
29	0.3	0.3	0.3	0.3	0.3	0.6	0.3	0.3	0.6	0.9	0.4	0.3	0.5
30	0.3	0.3	0.3	0.3	0.3	0.6	0.3	0.3	0.6	0.9	0.4	0.3	0.5
31	0.3	0.3	0.3	0.3	0.3	0.6	0.3	0.3	0.6	0.9	0.4	0.3	0.5
32	0.3	0.3	0.3	0.3	0.3	0.6	0.3	0.3	0.6	0.9	0.4	0.3	0.5
33	0.3	0.3	0.3	0.3	0.3	0.6	0.3	0.3	0.6	0.9	0.4	0.3	0.5
34	0.3	0.3	0.3	0.3	0.3	0.6	0.3	0.3	0.6	0.9	0.4	0.3	0.5
35	0.3	0.3	0.3	0.3	0.3	0.6	0.3	0.3	0.6	0.9	0.4	0.3	0.5
36	0.3	0.3	0.3	0.3	0.3	0.6	0.3	0.3	0.6	0.9	0.4	0.3	0.5

Table 18: Soil water retention capacity and critical z distance per soil class

Swrc[12] (-)	critical z distance(cm)	soil class
0.15	150	clay, calcareous
0.15	150	clay, non-calcareous
0.23	200	Loess
0.54	50	Peat
0.15	50	sand poor, non- calcareous
0.2	80	sand rich, non- calcareous
0.17	70	sand calcareous

[11] Decade (approx. 10 day period)
[12] Soil water retention capacity

Appendix 3 Available Chloride Analyses of Groundwater

Count of CL	year																								
Location - screen	69	75	76	77	78	79	80	81	82	83	84	85	86	87	88	89	90	91	92	93	94	95	96	97	98	Grand Total
EINI 394 1															1	1	1	1	1		1	1	1			8
EINI 394 2															1	1	1	1	1		1	1	1			8
HOVE PP IV 0																					1	1	1			3
HOVE PP IX 0																					1		1			2
HOVE PP V 0																					1	1	1			3
HOVE PP VI 0																					1	1	1			3
HOVE PP VII 0																					1	1	1			3
HOVE PP VIII 0																					1	1	1			3
NSTD 260 1								1	1		1	1	1	1	1	1	1	1	1	1	1	1	1			15
NSTD 260 2								1																		1
NSTD 260 3								1	1		1	1	1	1	1	1	1	1	1	1	1	1	1			15
PEY 259 1								1	1		1	1	1	1	1	1	1	1	1	1	1	1	1			15
PEY 259 2								1																		1
PEY 259 3								1	1		1	1	1	1	1	1	1	1	1	1	1	1	1			15
PEY PP IA 0																				1	1	1				3
PEY PP IIA 0																				1	1	1				3
PEY PP IIIA 0																				1	1		1			3
PEY PP IV 0																				1						1
PEY PP IVA 0																					1		1			2
PEY PP IX 0																				1	1	1				3
PEY PP V 0																				1	1		1			3
PEY PP VI 0																				1						1
PEY PP VIA 0																					1		1			2
PEY PP VII 0																				1	1		1			3
PEY PP VIII 0																				1	1		1			3
PEY PP X 0																				1	1	1				3
PEY PP XI 0																				1	1	1				3
PEY PP XII 0																				1	1	1				3
PEY WP 11 1																			1	4	1					6
PEY WP 11 2																			1	4	1					6
PEY WP 11 3																			1	4	1					6
PEY WP 11 4																			1	4	1					6
PEY WP 11 5																			1	4	1					6
REUT WP 1 4																			1							1
REUT WP 1 5																			1							1
ROOS 261 1								1	1		1	1	1	1	1	1	1	1	1	1	1	1				14
ROOS 261 2								1																		1
ROOS 261 3								1	1		1	1	1	1	1	1	1	1	1	1	1	1				14
ROOS GEZ RUW 0																		1						2		3
ROOS PP I 1		4	7	6	9	5	2																			33
ROOS PP II 1		2	2											1												5
ROOS PP IVA 0																		1								1
ROOS PP IX 0																						1		1		2
ROOS PP IXA 1																		1								1
ROOS PP IXA 2																		1								1
ROOS PP IXA 3																		1								1
ROOS PP V 0																						1		1		2
ROOS PP VI 0																						1		1		2
ROOS PP VI 1																								1		1
ROOS PP VII 0																								1		1
ROOS PP VII 1																								1		1
ROOS PP VIII 0																						1		1		2
ROOS PP VIII 1																								1		1
ROOS PP X 0																						1			5	6
ROOS WP 11 1										1		1													1	3
ROOS WP 11 2										1															1	2
ROOS WP 11 3										1															1	2
ROOS WP 12 1										1															1	2
ROOS WP 12 2										1															1	2
ROOS WP 12 3										1															1	2
ROOS WP 14 1																		5	4	1						10

ROOS	WP 15	1								1																1
ROOS	WP 15	2								1																1
ROOS	WP 16	1								1		1														2
ROOS	WP 16	2								1																1
ROOS	WP 16	3								1																1
ROOS	WP 17	1								1							1	1		1	1	1	1	1		8
ROOS	WP 17	2								1							1	1		1	1	1	1	1		8
ROOS	WP 18	1								1							1							1		3
ROOS	WP 19	1								1							1			1	1	1	1	1		7
ROOS	WP 20	1								1							1	1						1		4
ROOS	WP 21	1								1																1
ROOS	WP 21	2								1																1
ROOS	WP 22	1								1							5	4	1	1	1	1	1	1		16
ROOS	WP 22	2								1							5	4	1	1	1	1	1	1		16
ROOS	WP 22	3								1							5	4	1	1	1	1	1	1		16
ROOS	WP 23	1								1								1								2
ROOS	WP 23	2								1								1						1		3
ROOS	WP 28	1																						1		1
ROOS	WP 29	1															1	1					1			3
ROOS	WP 29	2															5	4	1	1	1	1	1	1		15
ROOS	WP 29	3															5	4	1	1	1	1	1	1		15
ROOS	WP 29	4															5	4	1	1	1	1	1	1		15
ROOS	WP 3	1																						1		1
ROOS	WP 30	1							2				5	1	2	1										11
ROOS	WP 31	1							1				5	1	2	1										10
ROOS	WP 32	1							1		1		5	1	2	1										11
ROOS	WP 33	1							1		1		5	1	2	1										11
ROOS	WP 34	1																		1	1		1			3
ROOS	WP 34	2															1			1	1	1	1	1		6
ROOS	WP 34	3															1			1	1	1	1	1		6
ROOS	WP 34	4															1									1
ROOS	WP 35	1															1		1							2
ROOS	WP 35	2															1		1							2
ROOS	WP 35	3															1		1							2
ROOS	WP 36	1															1									1
ROOS	WP 36	2															1									1
ROOS	WP 36	3															1									1
ROOS	WP 37	2															1									1
ROOS	WP 37	3															1									1
ROOS	WP 37	4															1									1
ROOS	WP 39	1															1									1
ROOS	WP 39	2															1									1
ROOS	WP 39	3															1									1
ROOS	WP 40	1															1		1	1	1	1	1	10		16
ROOS	WP 40	2															1		1	1	1	1	1	1		7
ROOS	WP 40	3															1		1	1	1	1	1	1		7
ROOS	WP 41	1																			1					1
ROOS	WP 41	2																			1			11		12
ROOS	WP 41	3																			1			2		3
ROOS	WP 41	4																			1			2		3
ROOS	WP 42	1																			1			3		4
ROOS	WP 42	2																						7		7
ROOS	WP 42	3																			1			1		2
ROOS	WP 43	1																		1				1		2
ROOS	WP 43	2																		1				2		3
ROOS	WP 43	3																		1						1
ROOS	WP 43	4																		1						1
ROOS	WP 43	5																		1						1
ROOS	WP 44	1																			1					1
ROOS	WP 44	2																			1					1
ROOS	WP 44	3																			1			1		2
ROOS	WP 45	1																			1					1
ROOS	WP 45	2																			1			1		2
ROOS	WP 45	3																			1					1
ROOS	WP 45	4																			1					1
ROOS	WP 46	1																			1					1
ROOS	WP 46	2																			1					1
ROOS	WP 46	3																			1					1
ROOS	WP 46	4																			1					1

ROOS	WP 46	5																				1				1
ROOS	WP 47	1																				1				1
ROOS	WP 47	2																				1				1
ROOS	WP 47	3																				1				1
ROOS	WP 48	1																				1				1
ROOS	WP 48	2																				1				1
ROOS	WP 48	3																				1				1
ROOS	WP 49	1																				1				1
ROOS	WP 49	2																				1				1
ROOS	WP 49	3																				1				1
ROOS	WP 49	4																				1				1
ROOS	WP 49	5																				1				1
ROOS	WP 6	1			1																					1
ROOS	WP 7	1			1																					1
ROOS	WP 74	1			1																					1
ROOS	WP 74	2			1																					1
ROOS	WP 74	3			1																					1
ROOS	WP 74	4			1																					1
ROOS	WP 74	5			1																					1
ROOS	WP 76	1										1														1
ROOS	WP 8	1	2																							2
ROOS	WP 9	1										1														1
ROOS	WP 95	1																							1	1
ROOS	WP 9A	1															1									1
ROOS	WP 9A	2															1									1
ROOS	WP 9A	3															1									1
SCHI	268	1								1	1	1	1	1	1	1	1	1	1							10
SCHI	268	2										1			1			1								3
SCHI	268	3								1	1	1	1	1	1		1	1								8
SCHI	418	1																			1	1	1			3
SCHI	418	2																			1	1	1			3
SCHI	PP IVA	0																		1	1	1				3
SCHI	PP VA	0																		1	1	1				3
SCHI	PP XII	0																		1	1	1				3
SCHI	PP XIII	0																		1	1	1				3
SCHI	PP XIV	0																		1	1	1				3
SCHI	PP XV	0																		1	1	1				3
SCHI	PP XVI	0																		1	2	1				4
SCHI	WP 13	1																	1							1
SCHI	WP 13	2																	1							1
SCHI	WP 13	3																	1							1
SCHI	WP 13	4																	1							1
SCHI	WP 13	5																	1							1
SITT	262	1														1	1	1			1	1	1			6
SUST	PP I	0																		1	1	1	1			4
SUST	PP II	0																		1	2	1	1			5
SUST	PP III	0																		1	1	1	1			4
SUST	PP IV	0																		1	1	1	1			4
SUST	PP IX	0																		1	1	1	1			4
SUST	PP V	0																		1	1		1			3
SUST	PP VI	0																		1	1		1			3
SUST	PP VII	0																		1	1		1			3
SUST	PP VIII	0																		1	1		1			3
SUST	PP X	0																		1	1	1	1			4
SUST	PP XI	0																		1	1	1	1			4
SUST	PP XII	0																		1	1	1	1			4
SUST	WP 4	1										1													1	2
SUST	WP 4	2										1														1
SUST	WP 5	1										1													1	2
SUST	WP 5	2										1														1
SUST	WP 5	3										1														1
SUST	WP 5	4										1														1
SUST	WP 6	1										1													1	2
SUST	WP 6	2										1														1
SUST	WP 6	3										1														1
SUST	WP 6	4										1														1
SUST	WP 7	1										1													1	2
SUST	WP 7	2										1														1
SUST	WP 7	3										1														1

SUST WP 7 4										1																1
Grand Total	2	6	9	13	9	5	2	14	6	27	22	33	12	17	14	10	11	78	57	70	75	86	47	26	75	##

Location - screen	69	75	76	77	78	79	80	81	82	83	84	85	86	87	88	89	90	91	92	93	94	95	96	97	98	

Appendix 4 Graphs of Transient Modelling Results

Appendix 5 Graphs of Simulated and Observed Chloride Concentrations

Appendix 6 Summary of Hydrological Features in the Model Area

Recharge

Average recharge in the model area is 300 mm/year. Within the model area such a recharge rate corresponds to 51 MM3/a. Minimal recharge occurred in 1976 (147 mm), maximal recharge in 1984 (539 mm). Over the period 1973 - 1996, no obvious trend in annual recharge rates can be distinguished.

River stages

Average river stage in the Meuse at river station Maaseik, near P.S. Roosteren, is 22.42 m NAP. The maximal stage observed at this station since 1973 is 29.40 m, in December 1993. Minimal values near 20.80 m. occurred frequently in many summers since 1973, as minimal river stages are controlled by weirs.

Drinking water production wells

Total annual well discharge rate for drinking water production within the model area varies between 4 and more than 15 million m3/year (MM3/a). Over the years, total extraction gradually increased to the maximal discharge rate in 1985. Since 1985, discharge rates were reduced; the average total extracted annual volume between 1986-1996 was almost 12 MM3/a. At P.S. Roosteren, pumping started in 1985 at a discharge rate of 5.8 MM3/a. After 1985, discharge rates were reduced and varied between 0 and 3 MM3/a, with an average of approximately 2 MM3/a.

Subsoil

Surface elevation varies in the greater part of the model area between 25 and 60 m NAP. The highest parts are located in the South part of the model area; the lowest areas are located along the riverbed of the Meuse. In the subsoil, there is no clear and distinct separation between aquifers and confining layers at scale of the model area, due to its highly heterogeneous character. Typically, in the NW of the model area, the top few meters consist of unsaturated clay, followed by 10 – 30 m of gravels and coarse sands, locally intersected by lenses of clay or brown coal. Below 0 m NAP, occurrence of clay and brown coal becomes more frequent and the thickness of the layers increases. According to available data, gravels only rarely occur in these deeper sections of the subsoil. Fine sands gradually become more frequent below 0 m NAP.

In the South-East part of the model area, eolian sediments dominate the upper sections of the subsoil. Lower sections consist of heterogeneously distributed sections of clays, sands and gravels.

Piezometric head and groundwater flow

Regional groundwater flow is directed NW to NNW. Within the model area, piezometric heads vary between 20 and 50 m NAP.

In subsoil sections of the North-West part of the model area, piezometric heads increase in downward direction. This implies that deep groundwater flows in upward direction in this part of the model area. Finally, these waters end up in the River Meuse. The magnitude of these fluxes depends strongly on vertical hydraulic resistance of the sub-soil sections below 0 m. NAP. These resistance values are relatively unknown, as few borehole descriptions of these sections are available. Possibly, substantial upward flow from subsoil sections below 0 m. NAP. would partly end up in pumped water at P.S. Roosteren.

Especially in the South-East part of the model area, piezometric heads in soil sections below 0 m. NAP decreased 3 – 5 m. between 1980 and 1992. The cause of this substantial decrease is thought to ly outside the model area of this study.

Part 2: Maps and Cross Sections

Map 1: Horizontal Dimensions of the Grid

Map 2: Vertical Dimensions of the Grid, Cross section A – A'

Map 3: Vertical Dimensions of the Grid, Cross section B – B'

Map 4: Location of Boreholes with Available Lithological Descriptions; Location of presented cross sections

Map 5: Sub-soil Composition: Cross Section A – A'

Map 6: Sub-soil Composition: Cross Section B – B'

Map 7: Sub-soil Composition: Cross Section C – C'

Map 8: Sub-soil Composition: Cross Section D – D'

Map 9: Sub-soil Composition: Cross Section E – E'

Map 10: Stationary Calibration: Weighted Errors for Layer 1

Map 11: Stationary Calibration: Average Weighted Errors for Layer 2 – 8

Map 12: Stationary Calibration: Weighted Errors for Layer 9

Map 13: Stationary Calibration: Weighted Errors for Layer 10

Map 14: Stationary Simulation: Caption Zones of P.S. Roosteren at Various Discharge Rates

Map 15: Stationary Simulation: Pathlines towards P.S. Roosteren, Cross section C – C'

Map 16: Stationary Simulation: Destinations of Particles Released at the Groundwater Table, Location of Cross Sections

Map 17: Stationary Simulation: Destinations of Particles Released at 15 m. NAP (Elevation of well screens of P.S. Roosteren)

Map 18: Stationary Simulation: Destinations of Particles Released at 0 m. NAP

Map 19: Stationary Simulation: Destinations of Particles Released at -50 m. NAP

Map 20: Stationary Simulation: Destinations of Particles Released at -120 m. NAP

Map 21: Stationary Simulation: Destinations of Particles Released along Cross Section A – A'

Map 22: Stationary Simulation: Destinations of Particles Released along Cross Section B – B'

Map 23: Transient Simulation: Location of Reference Points with Presented Time-Head Graphs

Map 24: Chloride: Monitoring Wells with Measured Chloride Concentrations

Map 25: Chloride: Average Observed Concentrations 1983 - 1984 along Cross Section A – A'

Map 26: Chloride: Average Observed Concentrations 1991 - 1993 along Cross Section A – A'

Map 27: Chloride: Average Observed Concentrations 1994 - 1996 along Cross Section A – A'

Map 28: Chloride: Average Observed Concentrations 1997 - 1998 along Cross Section A – A'

Map 29: Chloride: Average Observed Concentrations 1983 - 1984 along Cross Section B – B'

Map 30: Chloride: Average Observed Concentrations 1991 - 1993 along Cross Section B – B'

Map 31: Chloride: Average Observed Concentrations 1994 - 1996 along Cross Section B – B'

Map 32: Chloride: Average Observed Concentrations 1997 - 1998 along Cross Section B – B'

Map 33: Chloride: Average Observed Concentrations 1983 - 1984 along Cross Section C – C'

Map 34: Chloride: Average Observed Concentrations 1991 - 1993 along Cross Section C – C'

Map 35: Chloride: Average Observed Concentrations 1994 - 1996 along Cross Section C – C'

Map 36: Chloride: Average Observed Concentrations 1997 - 1998 along Cross Section C – C'

Map 37: Chloride: Average Observed Concentrations 1983 - 1984 along Cross Section D – D'

Map 38: Chloride: Average Observed Concentrations 1991 - 1993 along Cross Section D – D'

Map 39: Chloride: Average Observed Concentrations 1994 - 1996 along Cross Section D – D'

Map 40: Chloride: Average Observed Concentrations 1997 - 1998 along Cross Section D – D'

Map 41: Chloride: Average Observed Concentrations 1983 - 1984 along Cross Section E – E'

Map 42: Chloride: Average Observed Concentrations 1991 - 1993 along Cross Section E – E'

Map 43: Chloride: Average Observed Concentrations 1994 - 1996 along Cross Section E – E'

Map 44: Chloride: Average Observed Concentrations 1997 - 1998 along Cross Section E – E'

Map 45: Chloride: Average Concentrations along Cross Section F – F', 1983 - 1984

Map 46: Chloride: Average Concentrations along Cross Section F – F', 1991 - 1993

Map 47: Chloride: Average Concentrations along Cross Section F – F', 1994 - 1996

Map 48: Chloride: Simulated Concentrations along Cross Section F – F' in 2060